Bulletin du Service Géologique de l'Algérie
Vol. **34**, n° **1**, pp. **77-92**, **10** fig., **01** tabl., **2026**

PERRIERITE-(CE) IN THE ARCHEAN ALKALINE ORTHOGNEISS OF THE KHANFOUS AREA (IN OUZZAL TERRANE, NW HOGGAR)

Chakib HAROUZ[1], Khadidja OUZEGANE[2], and Sid Ali DOUKKARI[2]

ABSTRACT

Chevkinite-group minerals, including chevkinite-(Ce) and *perrierite-(Ce)*, are rare Fe–Ti silicates characterized by their ability to incorporate incompatible trace elements, particularly the light rare earth elements (LREE). The systematic LREE enrichment, coupled with restricted chemical variability, indicates crystallization of *perrierite-(Ce)* from differentiated alkaline magmas, with its primary chemical signature preserved during subsequent ultra–high-temperature metamorphism. This study presents new data on the occurrence and mineral chemistry of *perrierite-(Ce)* identified in high-grade alkaline orthogneisses from the Khanfous area in central Tekhamalt, located within the In Ouzzal terrane of the Western Hoggar (Algeria). The analyzed compositions confirm the presence of *perrierite-(Ce)*, with dominant LREE occupancy at the A site (Ce > La > Nd), Fe^{2+} at the B site, and Ti occupying both the C and D sites. The perrierite-(Ce) from Tekhamalt displays pronounced enrichment in LREE, with (La/Nd) ratios ranging from 2.1 to 6.4, and marked compositional heterogeneity. These findings provide important geochemical constraints on the stability and crystallization characteristic of chevkinite-group minerals under ultra–high-temperature metamorphic conditions.

Keywords - Perrierite - (Ce) - Orthogneiss - REE - Hoggar - Tekhamalt.

PERRIÉRITE-(CE) DES ORTHOGNEISS ALCALINS DE LA RÉGION DE KHANFOUS (TERRANE D'IN OUZZAL, HOGGAR OCCIDENTAL)

RÉSUMÉ

Les minéraux du groupe de la chevkinite, notamment la chevkinite-(Ce) et la perriérite-(Ce), sont des silicates ferrifères et titanifères rares capables d'incorporer d'importantes quantités d'éléments traces incompatibles, en particulier les terres rares légères (LREE). Leur enrichissement systématique en LREE, associé à une faible variabilité chimique, suggère une cristallisation de la perriérite-(Ce) à partir de magmas alcalins différenciés, dont la signature chimique primaire a été préservée au cours d'un métamorphisme ultérieur à très haute température. Cette

[1]Laboratoire Géoressources, Environnement et Risques Naturels (GEOREN), Université d'Oran 2 Mohamed Ben Ahmed, B.P. 1015 El M'naouer 31000 Oran, Algérie.

[2]Laboratoire de Géodynamique, Géologie de l'Ingénieur et de Planétologie, FSTGAT-U.S.T.H.B., B.P. 32 El Alia, Dar el Beida, 16111-Algiers, Algeria.

Auteur correspondant : Chakib HAROUZ. E-mail : harouz.chakib@univ-oran2.dz

- Manuscrit déposé sur l'ASJP le 31 juillet 2025, accepté après révision le 15 février 2026.*

**ASJP : Algerian Scientific Journal Platform.*

étude présente de nouvelles données sur la présence et la composition chimique de la perriérite-(Ce), identifiée dans des orthogneiss alcalins de haut grade de la région de Khanfous, au centre de Tekhamalt, au sein du terrane d'In Ouzzal, dans le Hoggar occidental (Algérie). Les analyses confirment la présence de la perriérite-(Ce), caractérisée par une prédominance des terres rares légères au site A (Ce > La > Nd), par la présence de Fe^{2+} au site B et de Ti aux sites C et D. La perriérite-(Ce) de Tekhamalt se distingue par un enrichissement marqué en terres rares légères, avec des rapports La/Nd compris entre 2,1 et 6,4, ainsi que par une hétérogénéité compositionnelle importante. Ces résultats apportent de nouvelles contraintes géochimiques sur la stabilité et les conditions de cristallisation des minéraux du groupe de la chevkinite dans un contexte de métamorphisme à très haute température.

Mots-clés - Perriérite-(Ce) - Orthogneiss - Terres rares - Hoggar - Tekhamalt.

I- INTRODUCTION

Chevkinite-(Ce) and perrierite-(Ce), the most common representatives of the chevkinite group, are typically found in alkaline rocks such as granites, syenites, rhyolites, carbonatites and fenites. They occur less frequently in gabbros and metacarbonates (MacDonald *et al*., 2012, 2013; Belkin *et al*., 2013). Perrierite, in particular, is stable under granulite-facies conditions (Grew and Manton, 1979a, 1979b, 1986; DePaolo *et al*., 1982; Harley, 1994; Hokada, 2007).

These minerals follow the general structural formula $A_4BC_2D_2Si_4O_{22}$, where A = REE, Ca, Sr, Th; B = Fe^{2+}; C = Ti, Al, Fe^{2+}, Mn, Mg, Zr, Nb; and D = Ti. To date, eleven species are recognized within the chevkinite group mineral (CGM) by the International Mineralogical Association - Commission on New Minerals, Nomenclature and Classification, reflecting significant structural and chemical diversity (MacDonald *et al*., 2012).

Despite their occurrence in a variety of geological environments, chevkinite-group minerals remain relatively rare in the geological record, due both to the specific geochemical conditions required for their formation and to their typically low modal abundance.

These minerals are of considerable geochemical interest owing to their strong affinity for rare earth elements (REE), particularly the light REE, with $\sum REE_2O_3$ contents reaching up to ~50 wt%. Their scarcity, combined with their ability to incorporate a wide range of trace elements, makes them valuable indicators of petrogenetic processes in both magmatic and high-grade metamorphic environments.

In this study, we report electron microprobe analyses of CGM identified in alkaline orthogneisses from the In Ouzzal terrane (Western Hoggar, Algeria). The aim is to refine the understanding of their compositional range in high-grade lithologies and to explore their geochemical signatures in relation to their host rocks.

II- GEOLOGICAL SETTINGS

The In Ouzzal terrane exhibits a lithological diversity and a crustal evolution, expressed by two main superposed units. The lower unit represents the lower crust and is dominated by high-grade enderbitic orthogneisses. These rocks derive from an Archean magmatic basement formed by the emplacement of TTG-type granitoids (tonalites, trondhjemites, and granodiorites) between 3.2 and 2.7 Ga. This early crust was subsequently intruded by alkaline granites at

2.65 Ga, likely in an extensional tectonic setting, and later by calc-alkaline granites around 2.5 Ga, generated by partial melting of tonalitic crust during the development of a dome-and-basin structural pattern (Peucat *et al*., 1996). The overlying unit consists of a supracrustal assemblage composed mainly of quartzites, marbles, calc-silicate rocks, and Al-Mg to Al-Fe granulites, locally associated with mafic to ultramafic lenses. All these granitoid protoliths with the supracrustal unit were ultimately metamorphosed under ultra-high-temperature conditions at approximately 2.0 Ga (Peucat *et al*., 1996; Ouzegane *et al*., 2003).

This study focuses on the Khanfous area in central Tekhamalt (figs. 1, 2). The Khanfous area extends over approximately 2 km in length and 500-900 m in width, forming a narrow, elongated strip oriented E-W to ENE-WSW. The complex comprises alkaline, clinopyroxene-bearing orthogneisses. These rocks enclose a varied assemblage of Al-Mg granulitic septum (fig. 2). Two main ithological units are identified. The first is a homogeneous, clinopyroxene-rich orthogneiss. The second is a supracrustal sequence associated with it. This sequence includes quartz-bearing Al-Mg granulites, notable for containing sapphirine-quartz-orthopyroxene-sillimanite and osumilite (Adjerid *et al*., 2008, 2013; Harouz *et al*., 2024). It also includes quartz-free Al-Mg granulites, magnetite-rich quartzites, garnet-pyroxenites, and marbles with olivine and spinel. Calc-silicate granulites are also present, characterized by the occurrence of fassaite (Harouz *et al*., 2024).

III- ALKALINE ORTHOGNEISS

The studied rock corresponds to the alkaline orthogneiss from the Khanfous area (fig. 3), previously described by Peucat *et al*. (1996), Ouzegane *et al*. (2003) and more recently by Harouz *et al*. (2024). Orthogneiss are interpreted as part of an alkaline magmatic suite ranging from

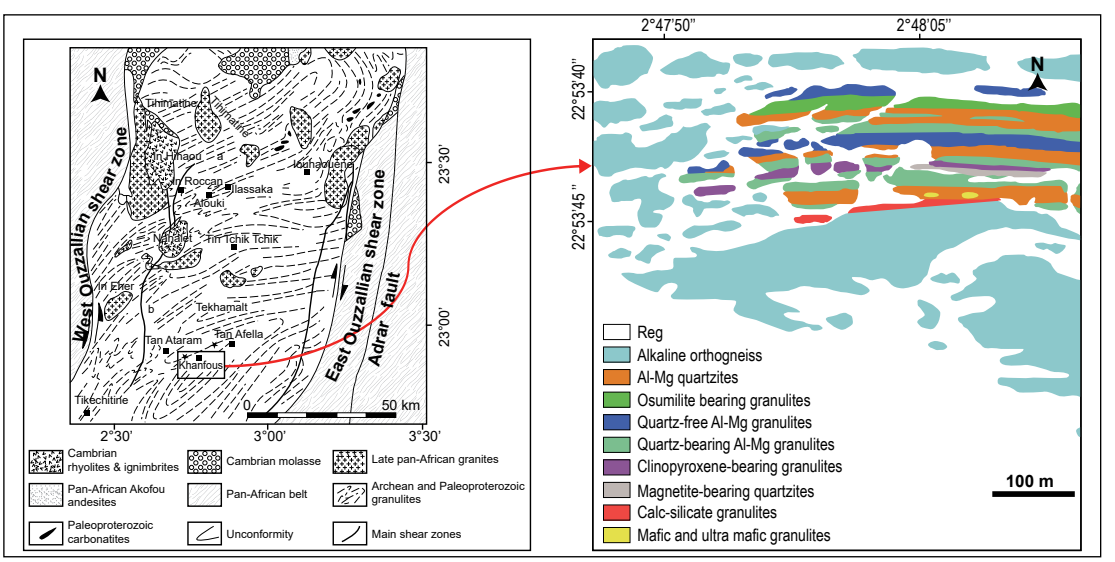


Fig. 1- Geological sketch map of the northern part of the In Ouzzal terrane (Caby, 1996).

Carte géologique de la partie nord du terrane d'In Ouzzal (Caby, 1996).

Fig. 2- Geological map of the Khanfous area (Adjerid *et al*., 2013); the star shows the location of the investigated samples.

Carte géologique de la région de Khanfous (Adjerid et al., 2013); l'étoile indique l'emplacement des échantillons étudiés.



Fig. 3- Orthogneiss outcrop in the Tekhamalt area.

Affleurement d'orthogneiss dans la région de Tekhamalt.

granodiorites and monzogranites to granites (Peucat *et al*., 1996), with SiO_2 contents between 69 and 75 wt.%. They are enriched in K_2O (6 wt.%) and incompatible elements (Ba >1000 ppm; Hf and Zr ~500-600 ppm), and exhibit low XMg ratios (0.07-0.11), indicating a rift-related A-type granite affinity (Eby, 1992; Peucat *et al*., 1996). REE patterns show moderate LREE enrichment ((La/Yb)N = 6-10) and flat HREE patterns ((Gd/Yb)N < 1.7). The orthogneisses are dated to around 2650 ± 10 Ma, placing them within the Archean evolution of the In Ouzzal terrane. This magmatism is characterized by metaluminous to slightly peraluminous, alkaline-type compositions. It is composed predominantly of quartz and perthitic feldspar, with clinopyroxene. The clinopyroxene shows a homogeneous composition, characterized by a very narrow range of XMg values (0.44-0.46). Al_2O_3 contents are constant, ranging from 1.15 to 1.28 wt%. The Ca, Mg, and Fe proportions (Ca 41-43, Mg 24-25, Fe 32-34) correspond to an iron-rich augite composition. (Rahmani, 1992; Harouz *et al*., 2024).

Quartz typically forms large anhedral aggregates, occasionally forming polycrystalline clusters. Perthitic textures are widespread in feldspars, reflecting high-temperature recrystallization. As accessory phases, numerous zircons, some apatites, and rare pyrites are present. Although petrographically similar to previously described samples, this study reveals that perrierite occurs as a large accessory phase, forming centimetre-scale, well-formed crystals disseminated within the quartz-feldspar matrix (fig. 4). While the presence of chevkinite had been noted in earlier studies (Acef *et al*., 2001, Ouzegane *et al*., 2003) their composition had not been investigated.

IV- MINERALOGY AND GEOCHEMICAL FEATURES

Representative analyses of the main mineral phases are reported in table 1 Chemical analyses were performed using a Cameca SX100 electron microprobe at the University of Paris VI. The operating conditions were 15 kV accelerating voltage and 20 nA sample current. The mineralogy and geochemistry of the perrierite were established through structural formula based on 22 oxygens, following the general formula $A_4BC_2D_2Si_4O_{22}$ (where A = Ca, REE, Th; B = Fe^{2+}; C = Fe^{2+}, Ti, Al, Mg, Mn, Nb; and D = Ti).

This normalization allows for accurate assessment of cation distribution among the crystallographic sites and provides a reliable basis for discussing the geochemical features and compositional variability of these minerals.

The most reliable criterion for distinguishing chevkinite from perrierite is the monoclinic β angle, which is approximately 100° in chevkinite and around 113° in perrierite (Haggerty and Mariano, 1983). In the absence of structural data, however, we employed the

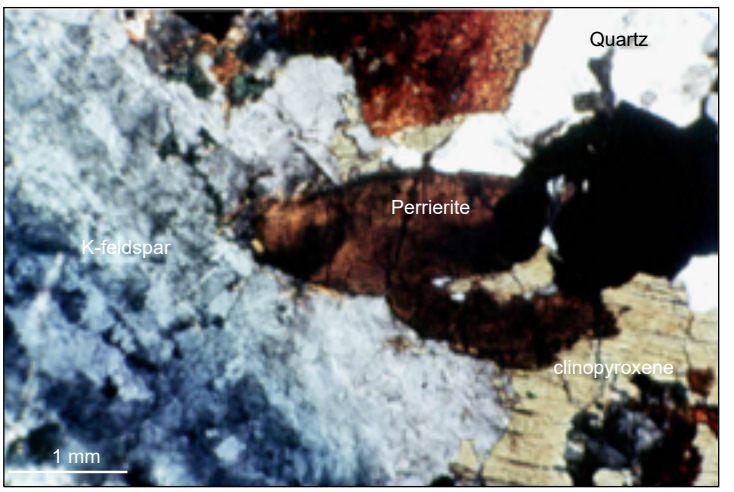


Fig. 4- Thin section photomicrograph of perrierite disseminated within the quartz-feldspar-clinopyroxene matrix of the Khanfous orthogneiss.

Photographie prise au microscope en lumière polarisée non analysée montrant la perriérite disséminée au sein de la matrice quartz–feldspath–clinopyroxène de l'orthogneiss de Khanfous.

empirical classification method proposed by MacDonald *et al*. (2009), which differentiates subgroup members based on a plot of total iron (expressed as FeO) versus CaO+SrO concentrations (see table 1 and fig. 5). According to this approach, all analyses from this study fall within the compositional field characteristic of perrierite.

This diagrammatic method also reflects the chemical differences associated with the structural dimorphism between chevkinite and perrierite, as outlined by Sokolova *et al*. (2004). Chevkinite typically exhibits higher concentrations of total iron (FeOT) and Ce_2O_3, whereas perrierite is relatively enriched in CaO and Al_2O_3.

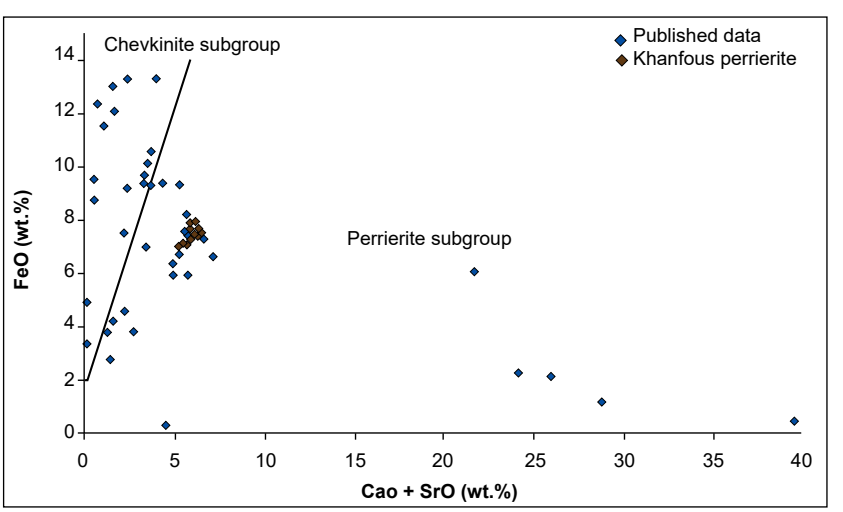


Fig. 5- Average analyses of perrierite-(Ce) from Khanfous, plotted in the FeO vs. (CaO + SrO) Classification Diagram of MacDonald *et al*. (2009), with supplemented data from published sources.

Analyses moyennes de la perriérite-(Ce) de Khanfous reportées sur le diagramme de classification FeO en fonction de (CaO + SrO) de Macdonald et al. (2009), complétées par des données issues de la littérature.

Table I- Representative electron microprobe analyses (values expressed in oxide wt.%) and mineral formulae for perrierite from Khanfous area (In Ouzzal terrane, Western Hoggar).

Analyses représentatives à la microsonde électronique (valeurs exprimées en %w.t) et formules structurales de la perriérite de la région de Khanfous (terrane d'In Ouzzal, Hoggar occidental).

	1	2	3	4	5	6	7	8	9	10	11	12	13
SiO_2	19.95	20.82	20.51	20.30	20.34	19.88	19.75	19.04	20.94	20.16	19.84	20.15	20.62
Al_2O_3	3.53	3.64	3.65	3.50	3.50	3.46	3.37	3.38	3.68	3.57	3.46	3.32	3.61
TiO_2	19.95	20.36	20.32	19.58	19.93	19.19	19.00	18.70	20.41	19.39	19.55	19.56	20.16
FeOt	7.35	7.66	7.55	8.14	8.02	7.99	7.95	6.97	7.67	7.42	7.48	7.15	7.58
MnOt	0.18	0.21	0.16	0.15	0.19	0.13	0.22	0.18	0.21	0.14	0.18	0.23	0.21
MgO	0.65	0.74	0.66	0.73	0.74	0.74	0.70	0.68	0.76	0.73	0.74	0.61	0.73
CaO	6.00	6.27	6.08	6.01	5.97	5.97	5.92	5.12	6.17	5.79	5.77	5.57	6.21
Eu_2O_3	0.00	0.00	0.00	0.00	0.00	0.00	0.00	0.00	0.00	0.00	0.00	0.00	0.00
SrO	Bdl	Bdl	Bdl	Bdl	Bdl	Bdl	Bdl	Bdl	Bdl	Bdl	Bdl	Bdl	Bdl
Na_2O	Bdl	Bdl	Bdl	Bdl	Bdl	Bdl	Bdl	Bdl	Bdl	Bdl	Bdl	Bdl	Bdl
ThO_2	3.16	3.91	3.05	3.46	3.43	3.68	3.85	2.06	3.51	3.17	3.55	3.02	3.87
La_2O_3	10.83	10.37	10.73	10.06	11.01	10.62	10.57	11.84	10.90	11.71	11.21	11.19	10.26
Ce_2O_3	16.35	16.79	16.88	16.57	17.04	15.53	15.75	19.31	16.98	17.13	16.62	16.87	16.63
Pr_2O_3	1.56	1.61	1.58	1.59	1.61	1.53	1.55	1.84	1.56	1.62	1.57	1.59	1.60
Nd_2O_3	3.69	3.58	3.69	3.78	3.78	3.55	3.49	4.55	3.46	3.90	3.37	3.67	3.55
Sm_2O_3	1.39	1.47	1.54	1.60	1.37	1.58	1.55	1.67	1.59	1.41	1.50	1.50	1.45
Gd_2O3	0.00	0.00	0.00	0.00	0.00	0.00	0.00	0.00	0.00	0.00	0.00	0.00	0.00
Dy_2O_3	0.39	0.39	0.31	0.43	0.40	0.42	0.45	0.37	0.37	0.39	0.38	0.36	0.39
Er_2O_3	0.00	0.02	0.00	0.00	0.01	0.00	0.00	0.00	0.00	0.00	0.00	0.00	0.02
Lu_2O_3	0.07	0.00	0.16	0.07	0.09	0.36	0.12	0.08	0.02	0.14	0.08	0.00	0.00
Nb_2O_5	0.81	0.92	0.84	1.23	1.16	1.25	1.23	0.64	0.76	0.92	1.01	0.79	0.91
Yb_2O_3	0.16	0.16	0.14	0.15	0.18	0.15	0.12	0.07	0.17	0.15	0.13	0.10	0.16
Ho_2O_3	0.37	0.39	0.45	0.44	0.40	0.43	0.54	0.31	0.45	0.48	0.34	0.38	0.39
Tb_2O_3	0.00	0.00	0.00	0.00	0.00	0.00	0.00	0.00	0.00	0.00	0.00	0.00	0.00
Ta_2O_5	0.05	0.00	0.01	0.07	0.14	0.00	0.00	0.07	0.00	0.00	0.00	0.03	0.00
ZrO_2	Bdl	Bdl	Bdl	Bdl	Bdl	Bdl	Bdl	Bdl	Bdl	Bdl	Bdl	Bdl	Bdl
TOTAL	**96.46**	**99.32**	**98.32**	**97.85**	**99.31**	**96.48**	**96.11**	**96.87**	**99.61**	**98.22**	**96.78**	**96.10**	**98.34**

Formula based on 22 oxygens						Formula based on 22 oxygens							
	1	2	3	4	5	6	7	8	9	10	11	12	13
La	0.790	0.732	0.766	0.725	0.786	0.778	0.780	0.887	0.768	0.848	0.820	0.822	0.732
Ce	1.184	1.177	1.196	1.185	1.207	1.130	1.154	1.437	1.186	1.231	1.208	1.231	1.177
Pr	0.113	0.113	0.111	0.113	0.113	0.111	0.113	0.136	0.109	0.116	0.113	0.116	0.113
Nd	0.260	0.245	0.255	0.264	0.261	0.252	0.250	0.330	0.236	0.274	0.239	0.261	0.245
Sm	0.095	0.097	0.103	0.108	0.091	0.108	0.107	0.117	0.104	0.096	0.103	0.103	0.097
Gd	0.000	0.000	0.000	0.000	0.000	0.000	0.000	0.000	0.000	0.000	0.000	0.000	0.000
Th	0.142	0.170	0.134	0.154	0.151	0.166	0.175	0.095	0.153	0.142	0.160	0.137	0.170
Ho	0.024	0.024	0.028	0.028	0.025	0.027	0.034	0.020	0.027	0.030	0.022	0.024	0.024
Lu	0.004	0.000	0.009	0.004	0.006	0.022	0.007	0.005	0.001	0.008	0.005	0.000	0.000
Yb	0.010	0.009	0.008	0.009	0.011	0.009	0.007	0.005	0.010	0.009	0.008	0.006	0.009
Dy	0.025	0.024	0.020	0.027	0.025	0.027	0.029	0.024	0.023	0.025	0.024	0.023	0.024
Ca	1.271	1.287	1.260	1.259	1.236	1.272	1.269	1.116	1.262	1.218	1.227	1.189	1.287
Sum A	3.917	3.878	3.890	3.875	3.912	3.901	3.924	4.172	3.879	3.997	3.928	3.912	3.878
Fe^{2+} (B)	1.000	1.000	1.000	1.000	1.000	1.000	1.000	1.000	1.000	1.000	1.000	1.000	1.000
Fe^{2+}	0.216	0.226	0.223	0.330	0.298	0.328	0.330	0.184	0.224	0.218	0.241	0.192	0.226
Mn	0.030	0.034	0.027	0.024	0.031	0.023	0.037	0.031	0.033	0.024	0.029	0.039	0.034
Mg	0.192	0.212	0.191	0.214	0.213	0.218	0.207	0.207	0.217	0.214	0.220	0.182	0.212
Nb	0.073	0.080	0.073	0.108	0.101	0.113	0.111	0.059	0.066	0.081	0.091	0.071	0.080
Ta	0.003	0.000	0.001	0.004	0.007	0.000	0.000	0.004	0.000	0.000	0.000	0.002	0.000
Ti	0.968	0.932	0.958	0.877	0.899	0.869	0.859	0.860	0.931	0.865	0.918	0.933	0.932
Al	0.824	0.822	0.833	0.805	0.798	0.809	0.794	0.809	0.828	0.826	0.808	0.779	0.822
Sum C	2.305	2.305	2.305	2.362	2.347	2.359	2.337	2.155	2.299	2.227	2.308	2.197	2.305
Ti (D)	2.000	2.000	2.000	2.000	2.000	2.000	2.000	2.000	2.000	2.000	2.000	2.000	2.000
Si	3.946	3.987	3.969	3.965	3.933	3.950	3.950	3.870	3.997	3.958	3.937	4.015	3.987
∑cations	12.145	12.203	12.157	12.190	12.140	12.127	12.137	12.076	12.176	12.085	12.101	12.072	12.203
∑REE	2.479	2.397	2.476	2.436	2.500	2.437	2.451	2.937	2.442	2.612	2.517	2.563	2.397
La/Ce	0.904	0.843	0.867	0.829	0.882	0.933	0.916	0.837	0.876	0.933	0.920	0.905	0.843
La/Sm	4.836	4.403	4.339	3.904	5.006	4.172	4.248	4.407	4.271	5.162	4.644	4.638	4.403
La/Nd	5.659	5.574	5.604	5.125	5.610	5.758	5.826	5.009	6.060	5.780	6.407	5.875	5.574
equ. O	22.000	22.000	22.000	22.000	22.000	22.000	22.000	22.000	22.000	22.000	22.000	22.000	22.000

The perrierite from Tekhamalt define a tight compositional cluster in the ternary Ti-Fe^{2+}-Al diagram (fig. 6), plotting distinctly toward the Ti-rich apex. This distribution reflects a marked dominance of Ti^{4+}, and is accompanied by comparatively low Fe^{2+} and moderate Al^{3+} contents. The average chemical formula of perrierite from the Khanfous area, normalized to 22 O, is: $(La_{0.787}Ce_{1.207}Pr_{0.114}Nd_{0.259}Sm_{0.102}Th_{0.149}Ho_{0.025}Lu_{0.005}Yb_{0.008}Dy_{0.025}Ca_{1.242})A(Fe^{2+})B(Fe_{0.248}Mn_{0.031}Mg_{0.207}Nb_{0.085}Ta_{0.002}Ti_{0.906}Al_{0.813})C(Ti_{2.000})D(Si_{3.979}O_{22})$

Compared to the chevkinite compositions described by Vlach and Gualda (2007) in the alkaline rocks of the Graciosa Province, the Khanfous orthogneisses show similar LREE and TiO_2 values but distinctly higher Al_2O_3 (~3.3-3.9 wt.% vs. <1 wt.% in Vlach and Gualda 2007). This difference may reflect a less peralkaline affinity. They also display high CaO contents, as expected for chevkinite-group minerals.

In the broader context of the chevkinite-group minerals, previously reported perrierite compositions (MacDonald and Belkin, 2002; MacDonald *et al*., 2009; MacDonald *et al*., 2019) show greater chemical variability, including several analyses enriched in Al (Al = 0.31-0.39 a.p.f.u. Al_2O_3 = 3.02-3.91 wt.%) that define a distinct trend toward the Al corner of the diagram. These Al-rich perrierite varieties contrast with the Ti-dominant character of the Tekhamalt samples (Ti = 3.31-4.55 a.p.f.u. TiO_2 = 16.35-19.47 wt.%), which form a chemically coherent subgroup.

All Tekhamalt compositions plot within the established compositional field of perrierite (fig. 6) and remain clearly distinct from chevkinite, which is typically characterized by higher Fe contents and lower Ti. Given that Fe^{2+} and Ti predominantly occupy the B and C/D crystallographic sites, respectively, the chemical variability observed within the analysis is largely governed by the distribution of these cations.

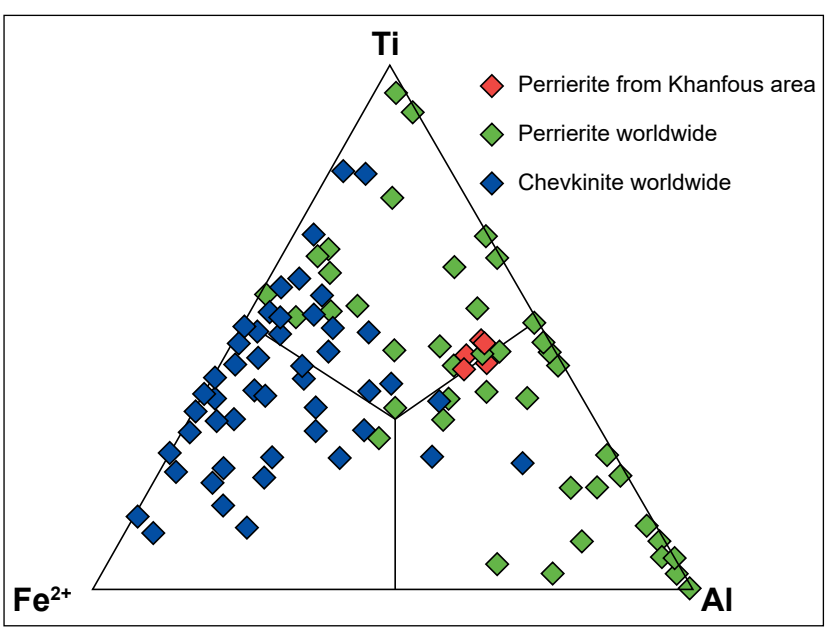


Fig. 6- Relative proportions of Fe^{2+}-Ti-Al in the C site of minerals of the chevkinite and perrierite subgroups. Perrierite from the Khanfous area is shown together with published data from Green & Pearson (1988) and MacDonald *et al*. (2019).

Proportions relatives de Fe^{2+}–Ti–Al dans le site C des minéraux des sous-groupes de la chevkinite et de la perriérite. Les données de la perriérite de la région de Khanfous sont présentées conjointement à celles publiées par Green et Pearson (1988) et MacDonald et al. (2019).

IV.1- "A site"

The A site in the studied samples is primarily occupied by LREE, notably Ce and La, accompanied by significant amounts of Ca. Cerium is overwhelmingly dominant in most analyses (up to 1.23 a.p.f.u), with La values ranging from 0.72 to 0.94 a.p.f.u. Ce_2O_3 remains the dominant REE in the majority of cases, with values ranging from 15.53 to 19.30 wt.% (table. 1). Such La enrichment, although not sufficient to redefine the species as perrierite-(La), is comparable to observations in La-rich perrierite from the Eifel volcanic district, Rheinland–Pfalz, Germany (Chukanov *et al*., 2012) or Golden Lake, Ontario (MacDonald *et al.,* 2009). However, none of the samples here reaches the atomic La/Ce ratio >1 observed in confirmed La-dominant varieties. Given the systematic Ce dominance, the studied minerals are classified as perrierite- (Ce). Neodyme is consistently present in moderate amount (0.23–0.33 a.p.f.u. Nd_2O_3 =3.36-4.55 w.t. %, table. 1), supporting the classification of these phases within LREE-dominant CGM. The Pr and Sm contents are lower but non-negligible (≈1.5 wt.%). The absence of reported Sr contents (presumably below detection) aligns with the broader trend in most perrierite/chevkinite analyses, with only rare exceptions (Bearpaw Mountains, Chakhmouradian and Mitchell, 1999).

New data for perrierite from the Khanfous orthogneisses plot on the REE–Ca–Sr diagram (fig. 7) within the low-Sr domain, clearly below 2.0 a.p.f.u. (Ca+Sr). This field is typically associated with metamorphic perrierite. The position of our samples within this field confirms their complete re-equilibration during the ultra-high-temperature metamorphic event at 2.0 Ga.

Furthermore, this overlap supports the view that the compositional gap between strontio-chevkinite and Sr-perrierite (2.0-2.5 a.p.f.u.) lacks a true crystallochemical basis and may be bridged by additional analyses from evolved or metasomatized lithologies (MacDonald *et al*., 2019).

A strong negative correlation is observed between (Ca + Sr) and total REE contents in

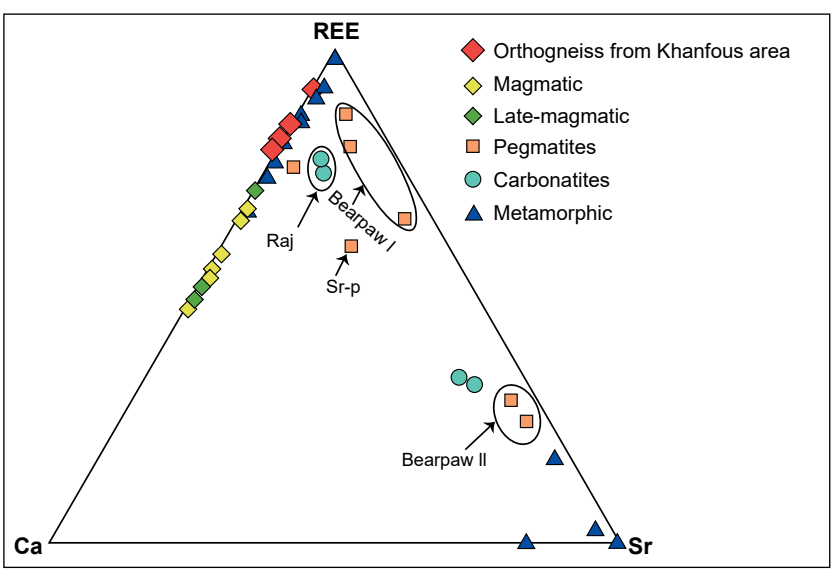


Fig. 7- REE–Ca–Sr diagram after MacDonald *et al*. 2009, with additional perrierite data from the Khanfous area . References for the compiled data are given in MacDonald *et al*. 2009.

Diagramme REE–Ca–Sr d'après MacDonald et al. (2009), incluant des données supplémentaires de perriérite provenant de la région de Khanfous. Les références des données compilées sont indiquées dans le Tableau 3 de MacDonald et al. (2009).

chevkinite-group minerals (r^2=0.69, MacDonald *et al*., 2002). For the Khanfous perrierite group, this relationship is even more pronounced, with r^2=0.97. The Khanfous perrierite grains (in red) plot toward the high-(Ca^+Sr), low-REE end of the trend, suggesting a strong substitution between large divalent cations (Ca^{2+}) and trivalent REE (fig. 8).

REE abundances in chevkinite-group minerals are overwhelmingly dominated by LREE, which is strongly expressed in the [La/Nd] ratios. Calculated [La/Nd] values range from 5 to 6.4, which is reflected in significant variation in the chondrite normalized REE patterns (fig. 9) with total REE contents ranging from approximately 33.7 to 39.7 wt.%. Most samples exhibit [La/Ce] ratios between 0.83 and 0.93, consistent with Ce typically exceeding La in chondrite-normalized patterns.

Overall, the composition of the A site in these samples is characteristic of REE-dominant CGM, with a clear LREE enrichment pattern, Ce > La > Nd > Sm, and with no evidence for Y- or Eu-dominant analogs such as those reported by Belkin *et al*. (2009) Perrierite-(Ce) from the Khanfous orthogneisses shows La/Nd ratios ranging from 5.0 to 6.4 and La/Ce ratios between 0.83 and 0.95 (table 1). The data define a relatively narrow compositional field with limited dispersion in La/Ce–La/Nd space. Compared to previously published datasets, the Khanfous perrierite compositions fall within the main range reported for natural perrierite but do not extend toward the extreme La/Nd values observed in some localities (fig. 9).

IV.2- "B" site

In the analyzed Tekhamalt perrierite-(Ce), the B site is fully occupied by Fe^{2+} (1.00 a.p.f.u. in all analyses), confirming the typical crystal-chemical configuration reported for most perrierite and chevkinite. No significant subs-

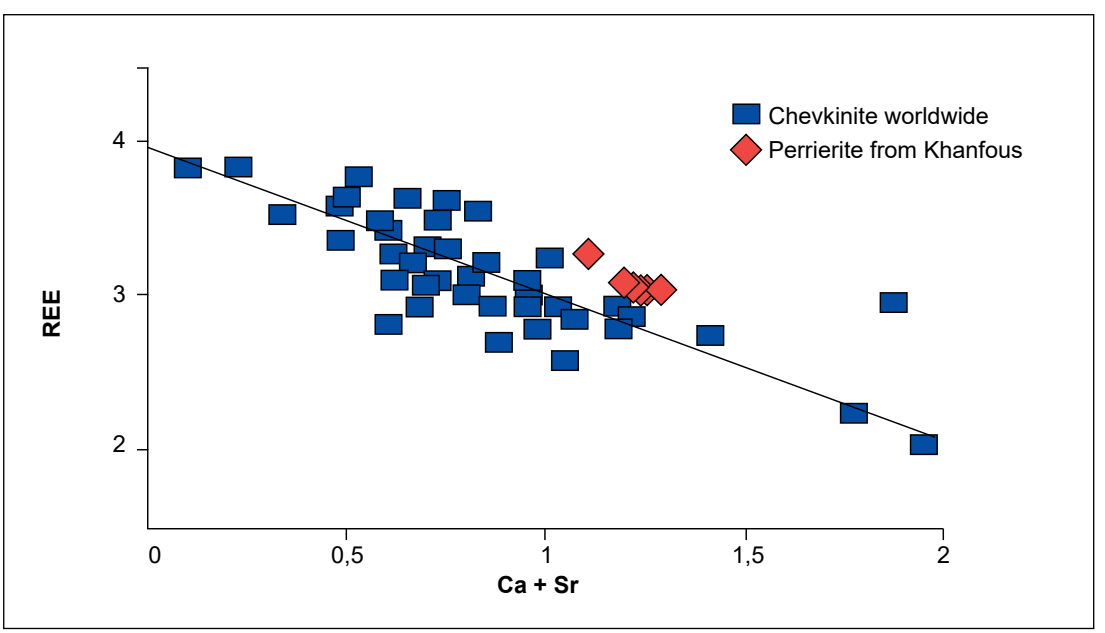


Fig. 8- Relationship between REE contents and (Ca+Sr) in the A site of chevkinite, perrierite, and c/p; modified after MacDonald *et al*. (2002) with additional perrierite data from Khanfous area.

Relation entre les teneurs en terres rares et (Ca+Sr) dans le site A de la chevkinite, de la perriérite et du groupe c/p ; modifié d'après MacDonald et al. (2002) avec ajout de données de perriérite de la région de Khanfous.

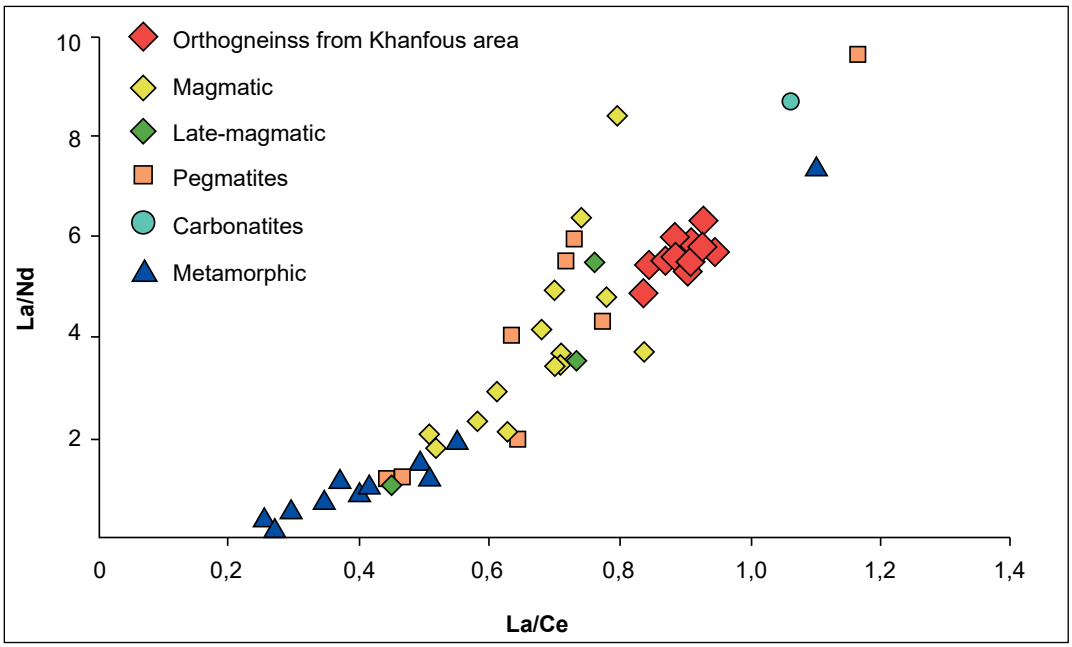


Fig. 9- Comparison of La/Nd and La/Ce ratios in perrierite from Tekhamalt Orthogneisses and various magmatic, pegmatitic, carbonatitic, and metamorphic rock types from MacDonald *et al*. (2009). "Carbonatites" refers to minerals associated with carbonatites (Sarambi, Paraguay – Haggerty & Mariano, 1983; Rajasthan, India – data compiled by MacDonald *et al*., 2009). Antarctica/India rocks in the "Metamorphic" group include associated pegmatites.

Comparaison des rapports La/Nd et La/Ce dans la perriérite des orthogneiss de Tekhamalt et dans divers types de roches magmatiques, pegmatitiques, carbonatitiques et métamorphiques, d'après MacDonald et al. (2009, compilation du Tableau supplémentaire 3). Le terme « carbonatites » désigne les minéraux associés aux carbonatites (Sarambi, Paraguay – Haggerty et Mariano, 1983 ; Rajasthan, Inde – données compilées par MacDonald et al., 2009). Les roches d'Antarctique et d'Inde incluses dans le groupe « Métamorphique » comprennent également des pegmatites associées.

titution by Mn or Mg is observed at this site, in contrast with Mg-rich perrierites from Antarctica (Harley, 1994) or Mn-dominant perrierite-(La) from India (Chukanov *et al*., 2012).

IV.3- "C" site

The C site is predominantly filled by Ti (0.86–0.97 a.p.f.u), accompanied by significant amounts of Al (0.80–0.93 a.p.f.u) and subordinate Fe^{2+} (0.18–0.33 a.p.f.u). This distribution confirms that Ti is the main occupant, while Al, although consistently present, does not reach dominance as reported in some Al-rich perrierites from Antarctica and India (Harley, 1994; Hokada, 2007; Belkin *et al*., 2009).

Minor constituents include Mg (0.18–0.25 a.p.f.u) and Mn (0.02–0.04 a.p.f.u), both of which remain below the levels reported for Mg- and Mn-rich analogues, such as the Antarctic perrierites with up to 0.77 a.p.f.u Mg (Harley, 1994; Hokada, 2007; Belkin *et al*., 2009) or Mn-rich varieties from India (Hokada, 2007). Similarly, Mn shows only minor variations and no clear correlation with other cations, consistent with its generally low abundance in perrierite-(Ce). Niobium is present at low levels (0.06–0.11 a.p.f.u).

The calculated cation sums for the C site (~2.30 a.p.f.u) fall well within the range re-

ported for chevkinite-group minerals (1.5–2.5 a.p.f.u; MacDonald *et al*., 2002), indicating neither strong site deficiency nor excess. This is in contrast to occurrences where A-site substitution into B or C sites induces significant deviations from the ideal formula.

IV.4- "D" site

The D site is filled by Ti.

IV.5-Perrierite substitution

A strong positive correlation between the Fe–Mn–Al group (dominantly occupying the C site) and Ca–Sr–Ti–Zr (distributed between the A and C sites) indicates a coupled substitution mechanism typical of the chevkinite group. This substitution is best described by the general exchange scheme $(Ca2+ + Sr2+)A + (Ti^{4+} + Zr^{4+})C = (REE,Y)^{3+}A + M^{2+,3+}C$, as originally proposed by Vlach & Gualda (2007) and MacDonald *et al*. (2019). The compositional trends observed in fig. 10 are fully consistent with this charge-balanced A–C site exchange.

The occurrence of Nb (0.06–0.11 a.p.f.u) in the C site may also indicate a secondary substitution mechanism of the form $Nb^{5+} + Fe^{2+} \leftrightarrow Ti^{4+} + Fe^{3+}$, as proposed by MacDo-

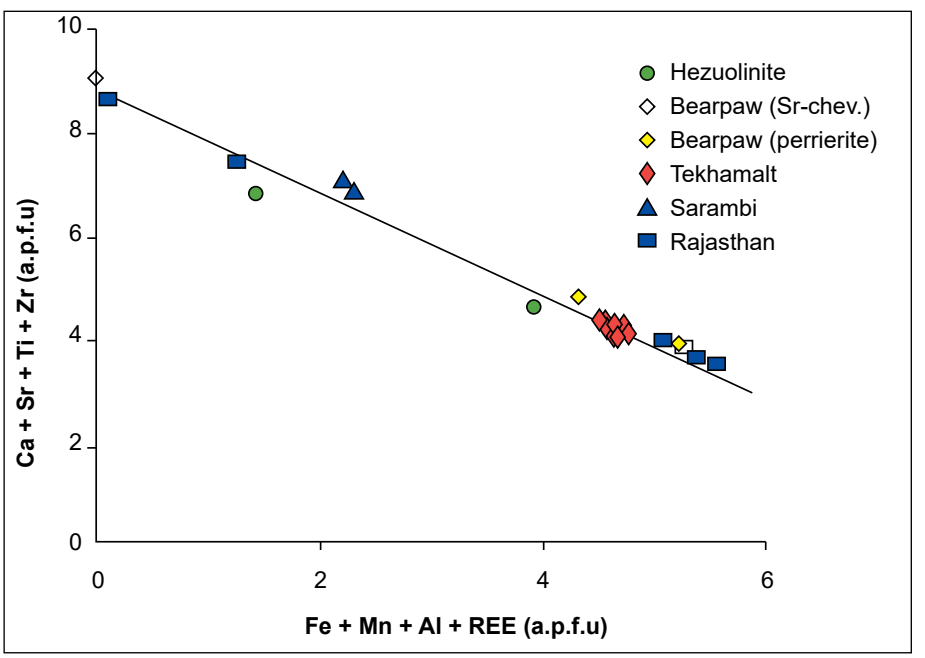


Fig. 10- Compositional variation in the Sr-rich members (SrO >2 wt.%) of the perrierite subgroup. Data sources are as follows: Sr- and Zr-rich perrierite-(Ce), Khanfous, Burpala massif, (MacDonald *et al*., 2012), Bearpaw Mountains (Chakhmouradian and Mitchell, 1999); rengeite, Japan, (Miyajima *et al*., 2001); matsubaraite, Japan (Miyajima *et al*., 2002); strontio-chevkinite, Sarambi, Paraguay (Haggerty and Mariano, 1983); Bayan Obo, China (Shimazaki *et al*., 2008); hezuolinite, Saima complex, China (Yang *et al*., 2011); Rajasthan, India (MacDonald *et al*., 2009).

Variations des termes riches en strontium (SrO > 2 % w.t) du sous-groupe de la perriérite. Les sources des données sont les suivantes : perriérite-(Ce) riche en Sr et Zr de Khanfous ; massif de Burpala (Macdonald et al., 2012) ; montagnes Bearpaw (Chakhmouradian et Mitchell, 1999) ; rengeite, Japon (Miyajima et al., 2001) ; matsubaraite, Japon (Miyajima et al., 2002) ; strontio-chevkinite, Sarambi, Paraguay (Haggerty et Mariano, 1983) ; Bayan Obo, Chine (Shimazaki et al., 2008) ; hezuolinite, complexe de Saima, Chine (Yang et al., 2011) ; Rajasthan, Inde (Macdonald et al., 2009).

nald *et al*. (2013). However, this interpretation remains tentative, as the Fe^{3+}/Fe^{2+} ratio in these samples has not been directly determined.

The presence of low but systematic Nb and trace Ta further supports the involvement of high field strength elements in the C site, consistent with observations for other perrierite-(Ce) occurrences.

In addition, as discussed for the A site, the observed inverse relationship between (Ca + Sr) and REE (fig. 8) further supports the classical substitution mechanism $[Ca^{2+} + Ti^{4+}] \leftrightarrow [REE^{3+} + Fe^{2+}/Al^{3+}]$ described for chevkinite-group minerals (MacDonald *et al*., 2002). This mechanism is consistent with the coupled exchanges identified in these samples.

V- CONCLUSION

The perrierite-(Ce) from the Khanfous orthogneisses crystallized from differentiated alkaline magmas enriched in LREE (up to 30%), consistent with the rift-related A-type granite affinity of their host rocks. Their chemistry is characterized by high TiO_2 contents (≈20 wt.%) and strong LREE enrichment, with La_2O_3 reaching ≈11wt.% and Ce_2O_3 from 15.53 to 19.31 wt.%.

Compared to the chevkinite compositions described by Vlach and Gualda (2007) in the alkaline rocks of the Graciosa Province, the Khanfous orthogneisses show similar LREE and TiO_2 values but distinctly higher Al_2O_3 (~3.3–3.9 wt.% vs. <1 wt.% in Vlach and Gualda 2007). This difference may reflect a less peralkaline affinity.

The observed compositional variability is primarily controlled by a charge-balanced coupled substitution mechanism involving the A and C crystallographic sites. A strong positive correlation between the Fe–Mn–Al group, dominantly occupying the C site, and Ca–Sr–Ti–Zr, distributed between the A and C sites, indicates a coupled A–C site exchange typical of the chevkinite group.

These values underscore the capacity of these minerals to concentrate REE to economically relevant levels, as chevkinite-group minerals are known accessory carriers of strategic elements. Such enrichment, coupled with elevated TiO_2 contents reinforces their significance both from a petrogenetic and resource perspective. Consequently, further investigations of other orthogneiss outcrop in the Tekhamalt region, including Tan Attaram, and Tan Affela, are recommended to assess their potential for CGM occurrence and to better constrain REE distribution in Archean alkaline terranes.

REFERENCES

ACEF, K., OUZEGANE, K., AND KIENAST, J.-R. 2001. Archean alkaline charnockitic gneisses in the In Ouzzal granulitic Unit West Hoggar, Algeria: evidence of pyrochlore and chevkinite. *Special Abstract Issue, EUG XI Strasbourg, France 571*.

ADJERID, Z., GODARD, G., OUZEGANE, K.-H., & KIENAST, J.-R. 2013. Multistage progressive evolution of rare osumilite-bearing assemblages preserved in ultrahigh-temperature granulites from in Ouzzal (Hoggar, Algeria). *Journal of Metamorphic Geology, 31*, 505–524. https://doi.org/10.1111/jmg.12031

ADJERID, Z., OUZEGANE, K., GODARD, G., & KIENAST, J.-R. 2008. First report of ultrahigh-temperature sapphirine+spinel+quartz and orthopyroxene+spinel+quartz parageneses discovered in Al–Mg granulites from the Khanfous area (In Ouzzal metacraton, Hoggar, Algeria). *Geological Society, London, Special Publications, 297* (1), 147–167. https://doi.org/10.1144/SP297.7

Adjerid, Z., Ouzegane, K., Godard, G., & Kienast, J.-R. 2008. Reactional history and phase relationships in ultrahigh-temperature sapphirine-spinel-quartz Al-Mg granulites from the Khanfous area in "The boundaries of the West African craton", Ennih, N. Liégeois, J-P. eds, *J. Geol. Soc. London*, Spe. Pub. 297.

Bagiński, B. & Macdonald, R. 2013. The chevkinite group: underestimated accessory phases from a wide range of parageneses. *Mineralogia, 44*(2–3), 3–18. doi:10.2478/mipo-2013-0006.

Belkin, H.-E., MacDonald, R., and Grew, E.-S. 2009. Chevkinite-group minerals from granulite-facies metamorphic rocks and associated pegmatites of East Antarctica and South India. *Mineralogical Magazine, 73,* 149–164.

Caby, R. 1996. A review of the In Ouzzal granulitic terrane (Tuareg shield, Algeria): its significance within the Pan-African Trans-Saharan Belt. *Journal of Metamorphic Geology, 14*, 659–666. doi:10.1111/j.1525-1314.1996.00048.x

Chakhmouradian, A.-R., and Mitchell, R.-H. 1999. Primary, agpaitic and deuteric stages in the evolution of accessory Sr, REE, Ba and Nb-mineralization in nephelinesyenite pegmatites at Pegmatite Peak, Bearpaw Mountains, Montana. *Mineralogy and Petrology, 67,* 85–110.

Chukanov, N.-V., Aksenov, S.-M., Rastsvelaeva, R.-K., Belakovskiy, D.-I., Göttlicher, J., Britvin, S.-N. and Möckel, S. 2012. Christofschäferite-(Ce), (Ce.La,-Ca)$_4$Mn^{2+} (Ti,Fe^{3+})$_3$(Fe^{3+},Fe^{2+},Ti)(Si$_2$O$_7$)$_2$O$_8$-a new chevkinite-group mineral from the Eifel area, Germany. *Novye Dannye o Mineralakh, 47*, 33–42.

Chukanov N.-V. *et al*. 2012. Perrierite-(La), (La, Ce, Ca)$_4$(Fe^{2+}, Mn)(Ti, Fe^{3+}, Al)$_4$ (Si$_2$O$_7$)$_2$O$_8$ a New Mineral Species from the Eifel Volcanic District, Germany. *Geology Of Ore Deposits* Vol. 54 ; N°8.

DePaolo, D.-J., Manton, W.-I., Grew, E.-S., & Halpern, M. 1982. Sm–Nd, Rb–Sr and U–Th–Pb systematics of granulite facies rocks from Fyfe Hills, Enderby Land, Antarctica. *Nature, 298*, 614–618. doi:10.1038/298614a0

Eby, G.-N. 1992. Chemical subdivision of the A-type granitoids: petrogenetic and tectonic implications. *Geology, 20*(7), 641–644. doi:10.1130/0091-7613(1992)020<0641>2.3.CO;2

Green, T.-H., and Pearson, N.-J. 1988. Experimental crystallization of chevkinite/ perrierite from REE-enriched silicate liquids at high pressure and temperature. *Mineralogical Magazine, 52*, 113–120.

Grew, E.-S., & Manton, W.-I. 1979a. Archean rocks in Antarctica: 2.5-billion-year uranium–lead ages of pegmatites in Enderby Land. *Science, 206*, 443–445.

Grew, E.-S., & Manton, W.-I. 1979b. Geochronologic studies in East Antarctica: age of a pegmatite in Mawson charnockite. *Antarctic Journal of the United States, 14*(5), 2–3.

Grew, E.-S., & Manton, W.-I. 1986. A new correlation of sapphirine granulites in the Indo-Antarctic metamorphic terrain: late Proterozoic dates from the Eastern Ghats Province of India. *Precambrian Research, 33*, 123–137.

Harley, S.-L. 1994. Mg-Al yttrian zirconolite in a partially melted sapphirine granulite, Vestfold Hills, East Antarctica. *Mineralogical Magazine, 58*, 259–269.

HAGGERTY, S.-E. AND MARIANO, A.-N. 1983. Strontianloparite and strontio-chevkinite: Two new minerals in rheomorphic fenites from the Parana Basin carbonatites, South America. *Contributions to Mineralogy and Petrology, 84*, 365-381.

HAROUZ, C., OUZEGANE, K., DOUKKARI, S., ADJERID, Z. AND AÏT-DJAFER, S. 2024. Metamorphic evolution and mineral assemblages of fassaite calc-silicate and sapphirine-quartz Al-Mg granulites from the Tekhamalt area (In Ouzzal terrane, Western Hoggar): Implications for ultra-high-temperature conditions and petrogeneses. *Journal of African Earth Sciences, 211*, 105184.

HAGGERTY, S.-E., AND MARIANO, A.-N. 1983. Strontian-loparite and strontio-chevkinite: Two new minerals in rheomorphic fenites from the Parana Basin carbonatites, South America. *Contributions to Mineralogy and Petrology, 84*, 365–381.

HOKADA, T. 2007. Perrierite in sapphirine–quartz gneiss: geochemical and geochronological features and implications for accessory-phase paragenesis of UHT metamorphism. *Journal of Mineralogical and Petrological Sciences, 102*, 44–49. doi:10.2465/jmps.060818

MACDONALD, R., MARSHALL, A.-S., DAWSON, J.-B., HINTON, R.-W., & HILL, P.-G. 2002. Chevkinite-group minerals from salic volcanic rocks of the East African Rift. *Mineralogical Magazine, 66*(2), 287–299. doi:10.1180/0026461026620029

MACDONALD, R., AND BELKIN, H.-E. 2002. Compositional variation in minerals of the chevkinite group. *Mineralogical Magazine, 66*, 1075–1098.

MACDONALD, R., BELKIN, H.-E., WALL, F., AND BAGIŃSKI, B. 2009. Compositional variation in the chevkinite group: new data from igneous and metamorphic rocks. *Mineralogical Magazine, 73*, 777–796.

MACDONALD, R., BAGIŃSKI, B., KARTASHOV, P., ZOZULYA, D., AND DZIERŻANOWSKI, P. 2012. Chevkinite-group minerals from Russia and Mongolia: new compositional data from fenites, metasomatites and ore deposits. *Mineralogical Magazine, 76*, 535–549.

MACDONALD, R., BAGINSKI, B., DZIER ZANOWSKI, P., FETTES, D.-J., AND UPTON, B.-G.-J. 2013. Chevkinite-group minerals in UK Palaeogene granites: underestimated REE-bearing accessory phases, Can. *Mineral., 51*, 333–347, https://doi.org/10.3749/canmin.51.2.333, 2013.

MACDONALD, R., BAGIŃSKI, B., BELKIN, H.-E., & STACHOWICZ, M. 2019. Composition, paragenesis and alteration of the chevkinite group of minerals. *American Mineralogist, 104*, 348-369.

MIYAJIMA, H., MATSUBARA, S., MIYAWAKI, R., YOKOYAMA, K., & HIROKAWA, K. 2001. Rengeite, $Sr_4ZrTi_4Si_4O_{22}$, a new mineral, the Sr–Zr analogue of perrierite from the Itoigawa–Ohmi district, Niigata Prefecture, central Japan. *Mineralogical Magazine, 65*(1), 111–120. doi:10.1180/002646101550163

MIYAJIMA, H., MIYAWAKI, R., & ITO, K. 2002. Matsubaraite, $Sr_4Ti_5(Si_2O_7)_2O_8$, a new mineral, the Sr–Ti analogue of perrierite in jadeitite from the Itoigawa–Ohmi district, Niigata Prefecture, Japan. *European Journal of Mineralogy, 14*(6), 1119–1128. doi:10.1127/0935-1221/2002/0014-1119

PEUCAT, J.-J., CAPDEVILA, R., DRARENI, A., CHOUKROUNE, P., FANNING, C.-M., BERNARD-GRIFFITHS, J., & FOURCADE, S. 1996. Major and trace element geochemistry and isotope (Sr, Nd, Pb, O) systematics of an Archaean basement involved in a 2.0 Ga very high-temperature (1000° C) metamorphic

event. In Ouzzal Massif, Hoggar, Algeria. *Journal of Metamorphic Geology, 14*(6), 667–692. https://doi.org/ 10.1111/j.1525-1314.1996.00054.x

Rahmani, A. 1992. Pétrologie et géochimie d'une série métasédimentaire dans le massif du Khanfous (In Ouzzal, Hoggar, Algérie). *Thèse de doctorat, Université Paris 6, France*.

Ouzegane, K., Kienast, J.-R., Bendaoud, A. and Drareni, A. 2003. A review of Archaean and Paleoproterozoic evolution of the In Ouzzal granulitic terrane (Western Hoggar, Algeria). *Journal of African Earth Sciences, 37*, 207–227. https://doi.org/10.1016/j.jafrea rsci.2003.05.002

Shimazaki, H., Yang, Z., Miyawaki, R., & Shigeoka, M. 2008. Scandium-bearing minerals in the Bayan Obo Nb–REE–Fe deposit, Inner Mongolia, China. *Resource Geology, 58*(1), 80–86. doi:10.1111/j.1751-3928.2007.00045.x

Sokolova, E., Hawthorne, F.-C., Della Ventura, G., and Kartashov, P.-M. 2004. Chevkinite-(Ce): crystal structure and the effect of moderate radiation-induced damage on site-occupancy refinement. *Canadian Mineralogist, 42*, 1013–1025.

Vlach, S.-R.-F., and Gualda, G.-A.-R. 2007. Allanite and chevkinite in A-type granites and syenites of the Graciosa Province southern Brazil. *Lithos, 97*, 98–121.

Yang, Z., Giester, G., Ding, K., & Tillmanns, E. 2012. Hezuolinite, $(Sr,REE)_4Zr(-Ti,Fe_3^+,Fe_2^+)_2Ti_2O_8(Si_2O_7)_2$, a new mineral species of the chevkinite group from Saima alkaline complex, Liaoning Province, NE China. *European Journal of Mineralogy, 24*(1), 189–196. doi:10.1127/0935-1221/2011/0023-2158